Vélez Rasero, Paris; Aznar Ballesta, Francisco; Coromina, Jan; [et al.]. «Compact coplanar waveguide power splitter with filtering capability based on slow-wave structures». Microwave and optical technology letters, Vol. 61, issue 5 (May 2019), p. 1143-1148. DOI 10.1002/mop.31671

Compact CPW power splitter with filtering capability based on slow-wave structures

P. Vélez[1], F. Aznar[2], J. Coromina[1], J. Bonache[1], and F. Martín[1]

[1] GEMMA/CIMITEC, Departament d'Enginyeria Electrònica, Universitat Autònoma de Barcelona, 08193 Bellaterra, Spain, E-mail: Ferran.Martin@uab.es

[2] Departamento de Teoría de la Señal y Comunicaciones, Universidad Politécnica de Madrid, 28031 Madrid, Spain, E-mail: Francisco.Aznar@upm.es

Abstract

A compact coplanar waveguide (CPW) power splitter with filtering capability is presented in this paper. The splitter consists of a pair of 70.71 Ω impedance inverters implemented by means of inductively and capacitively loaded slow-wave structures. Such slow-wave structures efficiently shorten the length of the inverters, thereby providing substantial size reduction to the power splitter. The filtering functionality is due to the Bragg effect, related to periodicity. The proposed splitter, designed to be functional at 1 GHz, exhibits good performance at that frequency, with measured return loss of 20.6 dB and insertion loss of 3.15 dB and 3.23 dB at the output ports. Moreover, the suppression level (at the output ports) at the first (3 GHz), second (5 GHz) and third (7 GHz) harmonic frequency is better than 12.4 dB, 34.6 dB and 24.7 dB, respectively. As compared to the length of the ordinary inverters, the length of the constitutive slow-wave impedance inverters of the designed power splitter is reduced by a factor of two.

Keywords: slow-wave structures, coplanar waveguides, power splitter

1. Introduction

Slow-wave transmission lines are artificial lines typically consisting of a host line periodically loaded with reactive elements [1,2]. The presence of reactive elements, e.g., shunt-connected capacitances [3-17], series-connected inductances [18-22], or a combination of both reactive elements [23-27], decreases the phase velocity of the line (slow-wave effect), thereby shortening the wavelength of the propagating signals. Therefore, these slow-wave artificial lines are useful for device miniaturization, since, for a required electrical length (dictated by design specifications), the physical length of such lines is shorter than the one of their ordinary counterparts. An additional property of such lines is the filtering capability, related to periodicity (Bragg effect) [2,28,29]. Namely, reactively loaded periodic lines exhibit pass bands and stop bands [30]. By properly designing the slow-wave transmission lines, it is possible to generate the rejection bands in frequency regions useful for harmonic or spurious suppression, and simultaneously obtain a behavior similar to the one of ordinary lines at lower frequencies (i.e., dispersion-less and all-pass functionality). Within these context, several works report compact microwave components with harmonic or spurious suppression capability [3-27,31-38].

Most slow-wave artificial lines and the corresponding (compact and eventually harmonic suppressed) microwave circuits have been implemented in microstrip technology [8,9,11,14,16,17,18,22,26,33,34], and only few of them have been designed and fabricated in coplanar waveguide (CPW) technology [1,20,25]. In [25], slow-wave CPW transmission lines based on simultaneous capacitive and inductive loading were reported. Such lines, applied to the design and fabrication of a compact and harmonic suppressed power splitter based on a single 35.35 Ω impedance inverter in [25], consist of a CPW line where the series inductances and shunt capacitances are implemented by means of slots in the ground plane and backside patches, respectively. In this paper, the main aim is to apply such slow-wave CPW transmission lines to the design of a power splitter with compact dimensions and filtering functionality, but alternatively to [25], based on a scheme where a pair of 70.71 Ω impedance inverters is considered. Consequently, the constitutive 90º (as corresponds to a quart-wavelength impedance inverter) and 70.71 Ω slow-wave lines are first designed, and then they are applied to the implementation of the power splitter. The fabrication and characterization results are presented in the last part of the paper.

2. Design of the slow-wave transmission lines

The topology and equivalent circuit model of the slow-wave transmission line (unit cell) are depicted in Fig. 1. The host line (a CPW) is loaded with a series inductance, L_{ls}, implemented by means of a pair of symmetric slots etched in the ground plane, and with a pair of shunt capacitances, $C_{ls}/2$, achieved by means of two patches etched in the back substrate side and connected to the central strip by means of a via. The host line is described by the characteristic impedance Z_0, and by the electrical length (kl), where k is the phase constant and l is the total (physical) length of the unit cell. Losses are excluded in the circuit model. As it was demonstrated in [25], the electrical length, βl, and the characteristic impedance, Z_B, of the loaded line, the two fundamental design parameters, are given by:

$$\cos(\beta l) = \cos(kl) - \left(\frac{L_{ls}}{2Z_0} + \frac{C_{ls}Z_0}{2}\right)\omega\sin(kl) - \frac{L_{ls}C_{ls}}{2}\omega^2\cos^2(kl/2) \tag{1}$$

$$Z_B = \frac{-jB}{\sin(\beta l)} \equiv \frac{Z_0\sin(kl) + \omega L_{ls}\cos^2(kl/2)}{\sin(\beta l)} \tag{2}$$

ω being the angular frequency. Note that from the previous two equations, the four unknowns (Z_0, kl, L_{ls} and C_{ls}) cannot be unequivocally determined. Indeed, an additional condition comes from the required size reduction of the slow-wave transmission line, determined by the so-called slow wave ratio, swr, defined by

$$swr = \frac{v_{pL}}{v_{po}} = \frac{\omega / \beta}{\omega / k} = \frac{kl}{\beta l} \quad , \tag{3}$$

where v_{pl} and v_{po} are the phase velocities of the loaded and unloaded lines, respectively. As it was pointed out in [25], the physical length of the slow wave transmission line, as compared to the one of the ordinary line, is dictated by the *swr*. Nevertheless, due to the finite size of the reactive elements loading the line, the actual length of the slow-wave transmission line is not as small as the value predicted by the *swr*.

From expression (3), once βl is set to a given value (dictated by design specifications), kl is directly obtained. The remaining parameters of the slow-wave transmission line, Z_0, L_{ls}, and C_{ls}, cannot be unequivocally determined from equations (1) and (2). However, extreme values of L_{ls}, and C_{ls}, that may prevent the implementation of such reactive components, must be avoided. In this regard, a trial-error approach is reasonable, where a guess value of Z_0 is provided and then L_{ls} and C_{ls} are isolated from (1) and (2). If such values are implementable, the value of Z_0 is considered to be the one to be synthesized (note, however, that Z_0 may be swept over a certain finite interval, yet providing implementable L_{ls} and C_{ls} values).

Another important aspect is the number of cells, N, of the considered slow-wave transmission line section. Obviously, it is intimately related to the electrical length of the unit cell, βl, which must be a submultiple of the total electrical length of the transmission line, designated as θ. In other words, $\theta = N \cdot \beta l$. Actually, the design parameter is θ (e.g., $\theta = \pi/2$ for an impedance or admittance inverter), rather than βl, but once N is set to a certain value, then βl is automatically determined. It was demonstrated in [25], and in other papers by the authors [14,26], that the preferred option to simultaneously leave the passband of interest unaltered and suppress the first harmonic bands in circuits based on transmission line impedance inverters, is to set $N = 2$. Therefore, this is the value adopted in this paper, as long as a harmonic suppressed power splitter based on a 70.71 Ω impedance inverter is pursued.

3. Synthesis of the slow-wave impedance inverter

The slow-wave transmission line to be synthesized is an impedance inverter with $\theta = \pi/2$, $Z_B = 70.71\ \Omega$ (the considered operating frequency has been set to $f_0 = 1$ GHz). Since $N = 2$ (see previous section), it follows that $\beta l = 45^o$. The slow wave ratio has been set to $swr = 0.5$, and, therefore, $kl = 22.5^o$. In regard to the remaining unknowns, Z_0, C_{ls} and L_{ls}, the characteristic impedance of the host line has been tentatively set to $Z_0 = 70\ \Omega$, providing the following reactive values: $C_{ls} = 0.93$ pF and $L_{ls} = 3.96$ nH. It has been found that such values can be easily implemented in CPW technology by means of the aforementioned backside patches and ground plane slots, respectively (hence these values of Z_0, C_{ls} and L_{ls} have been considered to be definitive).

In order to generate the unit cell layout, the slot dimensions providing the required inductance value, as well as the dimensions of the transverse backside patches necessary to achieve the shunt capacitance, have been independently determined. Nevertheless, some post-optimization has been necessary in order to adjust the characteristic impedance and electrical length to the design values at the operating frequency. The resulting layout of the unit cell is the one depicted in Fig. 1. The characteristic impedance and the electrical length of the unit cell, inferred by electromagnetic simulation of the layout by means of *Keysight Momentum*, are depicted in Fig. 2, where it is apparent that the required values at f_0 (i.e., Z_B = 70.71 Ω and βl = 45º) are achieved. By concatenating two cells, we do expect that θ = 90º at f_0, as Fig. 3 corroborates. In such figure, the transmission and reflection coefficients, referred to a 50 Ω port impedance, are also depicted. Moreover, we have included in Fig. 3 (and in Fig. 2) the corresponding curves obtained through circuit simulation of the equivalent circuit model, and the agreement is excellent up to roughly 4.5 GHz, i.e., clearly above f_0. At higher frequencies, the disagreement is because the patch capacitance and inductive slots can no longer be considered semi-lumped components. In the previous electromagnetic simulations, the considered substrate is *Rogers RO3010* with thickness h = 1.27 mm, dielectric constant ε_r = 10.2 and loss tangent tanδ = 0.0023.

4. Fabrication of the power splitter and experimental results

The layout and the photograph of the designed slow-wave power splitter are depicted in Fig. 4 (notice that air-bridges, implemented by means of backside strips and vias, have been used in order to suppress the parasitic CPW slot mode). Fig. 5 depicts the return loss (S_{11}) and power splitting (S_{21} and S_{31}) of the divider, inferred from circuit, electromagnetic simulation (with and without losses) and measurement. The designed slow-wave power splitter has been fabricated by means of a *LPKF-H100* drilling machine, and the measured response has been obtained by means of the *Keysight PNA 5221A* vector network analyzer. The response of the slow-wave power splitter is roughly the same than the one of the ordinary splitter in the region of interest (vicinity of f_0), also included in Fig. 5(a). Particularly, S_{21} = –3.15 dB, S_{31} = –3.23 dB and S_{11} = –20.6 dB at f_0 (measured values). However, the first (at $3f_0$), second (at $5f_0$), and third (at $7f_0$) harmonic bands of the conventional splitter are significantly suppressed in the slow-wave implementation, i.e., the measured suppression levels for port 2 have been found to be 12.4 dB, 34.6 dB and 34.3 dB, respectively, and 12.7 dB, 42.6 dB and 24.7 dB, respectively, for port 3. With these results, it is clearly demonstrated that the proposed strategy, based on replacing the ordinary inverter of the splitter with a slow-wave transmission line, is useful to achieve power splitting and filtering simultaneously. Moreover, the filtering action provides significant levels of harmonic suppression. Indeed, the achieved stopband region (considering a suppression level of at least 10 dB) extends up to at least $7f_0$, superior than in the splitter reported in [25].

Concerning splitter dimensions, these are mainly determined by the length of the synthesized slow-wave impedance inverter. The actual ratio between the length of the designed inverter and the ordinary counterpart (implemented by means of a conventional 90º line) is 0.505, i.e., slightly superior that the theoretical value given by the considered *swr* (for the reasons explained above). However, the achieved size reduction of the inverter is very close to the nominal value, hence providing a small size to the fabricated splitter.

5. Conclusions

In conclusion, a compact and harmonic suppressed CPW power splitter based on a pair of slow-wave transmission line 70.71 Ω impedance inverters has been designed and fabricated. Roughly 50% length reduction in the inverters has been achieved (as compared to the length of the ordinary CPW inverters), and the fabricated splitter has been demonstrated to efficiently reject at least the first three harmonic bands, leaving the response in the region of interest unaltered. It has been shown that the proposed circuit model of the slow-wave transmission line inverter, useful for design purposes, provides a good description of the behavior of the splitter in the region of interest, and such good agreement between the circuit and the electromagnetic responses extends up to $4.5f_0$.

Acknowledgments

This work was supported in part by MINECO-Spain under Project TEC2016-75650-R, in part by Generalitat de Catalunya (project 2017SGR-1159), in part by the Institució Catalana de Recerca i Estudis Avançats (who awarded F. Martín), and in part by FEDER funds.

References

1. K. Wu, “Slow wave structures,” in *Encyclopedia of Electrical and Electronics Engineering*, J. G. Webster, Ed. New York: Wiley, 1999, vol. 19, pp. 366–381.
2. F. Martín, *Artificial Transmission Lines for RF and Microwave Applications*, John Wiley, Hoboken (NJ), 2015.
3. T. Hirota, A. Minakawa, M. Muraguchi, “Reduced-size branch-line and rat-race hybrids for uniplanar MMIC's”, *IEEE Trans. Microw. Theory Techn*., vol. 38, pp. 270-275, Mar 1990.
4. A. Görür, “A novel coplanar slow-wave structure,” *IEEE Microw. Guided Wave Lett*., vol. 4, pp. 86–88, 1994.
5. A. Görür, C. Karpuz and M. Alkan, “Characteristics of periodically loaded CPW structures”, *IEEE Microw. Guided Wave Lett*., vol. 8, pp. 278-280, 1998.
6. R. B. Singh and T. M. Weller “Miniaturized 20 GHz CPW quadrature coupler using capacitive loading”, *Microw. Opt. Technol. Lett*., vol. 30, pp. 3-5, Jul. 2001.
7. M. C. Scardelletti, G. E. Ponchak, and T. M. Weller, “Miniaturized Wilkinson power dividers utilizing capacitive loading”, *IEEE Microw. Wirel. Compon. Lett*., vol. 12, pp. 6-8, Jan. 2002.
8. K. W. Eccleston and S.H.M. Ong, “Compact planar microstripline branch-line and rat-race couplers”, *IEEE Trans. Microw. Theory Tech*., vol. 51, pp 2119-2125, 2003.
9. J. García-García J. Bonache and F. Martín, “Application of electromagnetic bandgaps (EBGs) to the design of ultra-wide band pass filters (UWBPFs) with good out-of-band performance”, *IEEE Trans. Microw. Theory Tech*., vol. 54, pp. 4136-4140, 2006.
10. C-I. Shie, J-C. Cheng, S-C. Chou, and Y-C. Chiang, “Transdirectional Coupled-Line Couplers Implemented by Periodical Shunt Capacitors”, *IEEE Trans. Microw. Theory Tech*., vol. 57, pp. 2981-2988, Dec. 2009.

11. H. Cui, J. Wang and J.-L. Li, “Compact Microstrip Branch-line Coupler with Wideband Harmonic Suppression”, *ACES Journal*, vol. 27, pp. 766-771, Sep. 2012.
12. M. Orellana, J. Selga, M. Sans, A. Rodríguez, V. Boria, F. Martín, “Synthesis of slow-wave structures based on capacitive-loaded lines through Aggressive Space Mapping (ASM)”, *Int. J. RF Microw. Comp. Aided Eng.*, vol. 25, pp. 629-638, Sep. 2015.
13. J. Selga, P. Vélez, M. Orellana, A. Rodríguez, V. Boria, F. Martín, “Size reduction and spurious suppression in microstrip coupled line bandpass filters by means of capacitive electromagnetic bandgaps”, *IEEE MTT-S Int. Microw. Symp*. (IMS’16), San Francisco, CA, 22-27 May 2016.
14. M. Orellana, J. Selga, P. Vélez, A. Rodríguez, V. Boria, F. Martín, “Design of capacitively-loaded coupled line bandpass filters with compact size and spurious suppression”, *IEEE Trans. Microw. Theory. Techn.*, vol. 65, pp. 1235-1248, Apr. 2017.
15. J. Selga, J. Coromina, P. Vélez, F. Martín, “Application of electromagnetic bandgaps based on capacitively-loaded lines to the reduction of size and suppression of harmonic bands in microwave devices”, *IEEE MTT-S International Conference on Numerical Electromagnetic and multiphysics Modeling and Optimization for RF, Microwave and Terahertz Applications* (NEMO), May, 17-19, 2017, Sevilla, Spain.
16. J. Coromina, J. Selga, P. Vélez, J. Bonache, F. Martín, “Size reduction and harmonic suppression in branch line couplers implemented by means of capacitively-loaded slow-wave transmission lines”, *Microw. Opt. Technol. Lett.*, vol. 59, pp. 2822–2830, 2017.
17. J. Coromina, J. Selga, P. Vélez, J. Bonache and F. Martín, “Slow-wave artificial transmission lines based on stepped impedance shunt stub (SISS) loading: analysis and stopband bandwidth enhancement”, *48th European Microwave Conference*, Madrid, Spain, Sep., 2018.
18. L. Zhu, “Guided-wave characteristics of periodic microstrip lines with inductive loading: slow-wave and bandstop behaviors”, *Microw. Opt. Techn. Lett*., vol. 41, pp. 77-79, 2004.
19. S. Lee and Y. Lee, "Generalized miniaturization method for coupled-line bandpass filters by reactive loading", *IEEE Trans. Microw. Theory Techn*., vol. 58, no.9, pp. 2383-2391, Sep. 2010.
20. P. Vélez, J. Selga, J. Bonache and F. Martín, “Slow-wave inductively-loaded electromagnetic bandgap (EBG) coplanar waveguide (CPW) transmission lines and application to compact power dividers”, *Europ. Microw. Conf.*, London (UK), 3-7 Oct. 2016.
21. J. Selga, P. Vélez, J. Bonache, and F. Martín, “EBG-based transmission lines with slow-wave characteristics and application to miniaturization of microwave components”, *Appl. Phys. A*, vol. 123, p. 44, 2017.
22. J. Selga, J. Coromina, P. Vélez, A. Fernández-Prieto, A. J. Martínez-Ros, Jordi Bonache, F. Aznar-Ballesta, and F. Martín, “Compact Power Splitter with Harmonic Suppression based on Inductively-Loaded Slow-Wave Transmission Lines”, *Microw. Opt. Technol. Lett.*, vol. 60, pp.1464–1468, Jun. 2018.
23. H. M. Liu, S. J. Fang, Z. B. Wang, and Y. Zhou, “Miniaturization of trans-directional coupled line couplers using series inductors”, *Prog. Electromagn. Research C*, vol. 46, pp. 171-177, 2014.
24. J. Selga, P. Vélez, J. Bonache, F. Martín, “High miniaturization potential of slow-wave transmission lines based on simultaneous inductor and capacitor loading”, *European Microwave Conference*, Nuremberg, Germany, Oct. 2017.
25. F. Aznar-Ballesta, J. Selga, A. Fernández-Prieto, J. Coromina, P. Vélez, J. Bonache, F. Martín, “Slow wave coplanar waveguides based on inductive and capacitive loading and application to compact and harmonic suppressed power splitters”, *International Journal of Microwaves and Wireless Technologies*, vol. 10, pp. 530-537, Jun. 2018.

26. J. Selga, P. Vélez, J. Coromina, A. Fernández-Prieto, J. Bonache, and F. Martín, "Compact branch-line coupler implemented by means of slow-wave transmission lines based on simultaneous inductive and capacitive loading", *Microw. Opt. Technol. Lett.*, to be published.
27. J. Selga, J. Coromina, P. Vélez, A. Fernández-Prieto, J. Bonache, and F. Martín "Miniaturized and harmonic-suppressed rat-race couplers based on slow-wave transmission lines", *IET Microw., Ant. Propag.,* under review.
28. E. Yablonovitch, "Photonic band gap structures", *J. Opt. Soc. Amer.* B 10, pp. 283-295, 1993.
29. J. D. Joannopoulos, R. D. Meade, and J. N. Winn, *Photonic Crystals: Molding the Flow of Light*, Princeton, NJ, Princeton University Press, 1995.
30. F. Martín, F. Falcone, J. Bonache, M.A.G. Laso, T. Lopetegi, M. Sorolla, "Dual electromagnetic bandgap CPW structures for filter applications", *IEEE Microw. Wireless Compon. Lett.*, vol. 13, pp. 393-395, 2003.
31. M-L. Chuang, "Miniaturized ring coupler of arbitrary reduced size", *IEEE Microw. Wirel. Compon. Lett*., vol. 15, pp. 16-18, Jan. 2005.
32. S-S. Liao, P-T. Sun, N.-C. Chin, and J-T. Peng, "A Novel Compact-Size Branch-Line Coupler", *IEEE Microw. Wireless Compon. Lett*., vol. 15, pp. 588-590, Sep. 2005.
33. J. Gu, and X. Sun, "Miniaturization and harmonic suppression of branch-line and rat-race hybrid coupler using compensated spiral compact microstrip resonant cell", *IEEE MTT-S Int. Microw. Symp*. (IMS'05), Los Angeles, CA, Jun. 2005.
34. S.-S. Liao, and J.-T. Peng, "Compact planar microstrip branch-line couplers using the quasi-lumped elements approach with nonsymmetrical and symmetrical T-shaped structure", *IEEE Trans. Microw. Theory Techn*., vol. 54, pp. 3508-3514, Sep. 2006.
35. J. Wang, B.-Z. Wang, Y.-X. Guo, L. C. Ong, and S. Xiao," A compact slow-wave microstrip branch-line coupler with high performance", *IEEE Microw. Wirel. Compon. Lett.*, vol. 17, pp. 501-503, Jul. 2007.
36. P. Mondal A. Chakrabarty, "Design of miniaturised branch-line and rat-race hybrid couplers with harmonics suppression", *IET Microw. Antennas Propag*., vol. 3, pp. 109–116, 2009.
37. V. K. Velidi, B. Patel, S. Sanyal, "Harmonic suppressed compact wideband branch-line coupler using unequal length open-stub units", *Int. J. RF Microw. Comput.-Aid. Eng.*, vol. 21, pp. 115-119, Jan. 2011.
38. S. Koziel and P. Kurgan, "Low-cost optimization of compact branch-line couplers and its application to miniaturized Butler matrix design," *44th European Microwave Conference*, 6-9 Oct. 2014, Rome (Italy), pp. 227-230.

Figures

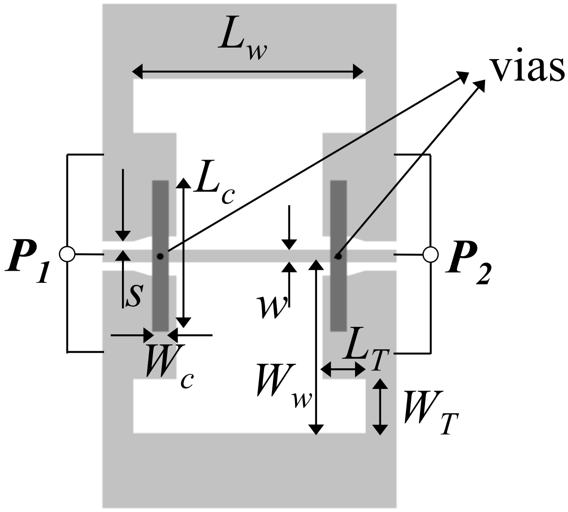

(a)

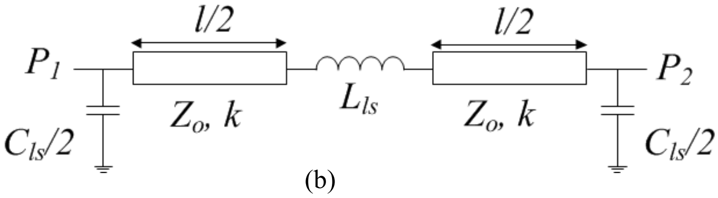

(b)

Fig. 1. Topology (unit cell) (a) and circuit schematic (b) of the slow wave CPW transmission line.

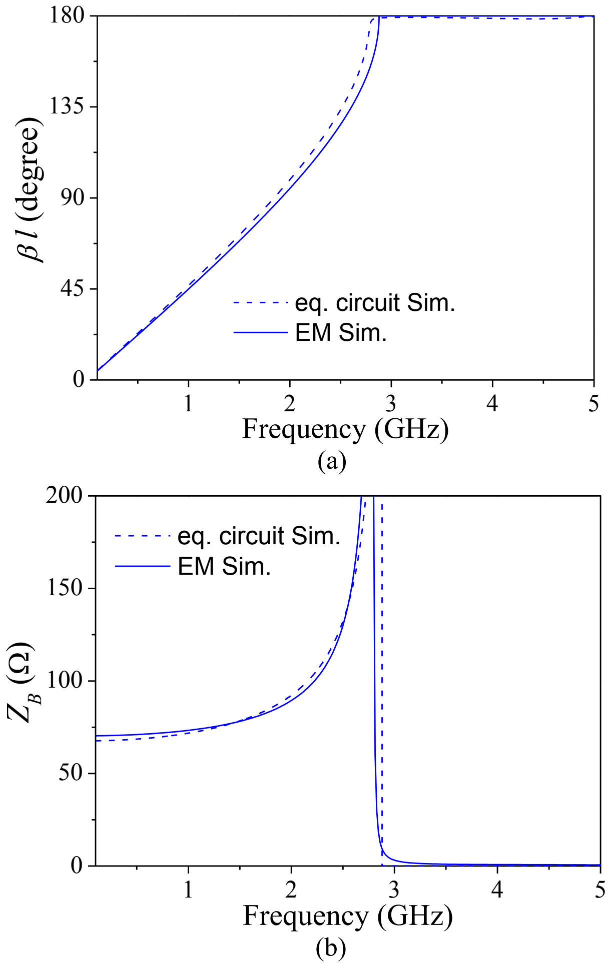

Fig. 2. Electrical length (a) and characteristic impedance (b) of the inverter unit cell. Dimensions are (in reference to Fig. 1): L_w = 7.00 mm, W_w = 5.00 mm, L_T = 1.30 mm, W_T = 1.63 mm, L_C = 4.55 mm, W_C = 0.50 mm, w = 0.38 mm, s = 0.40 mm.

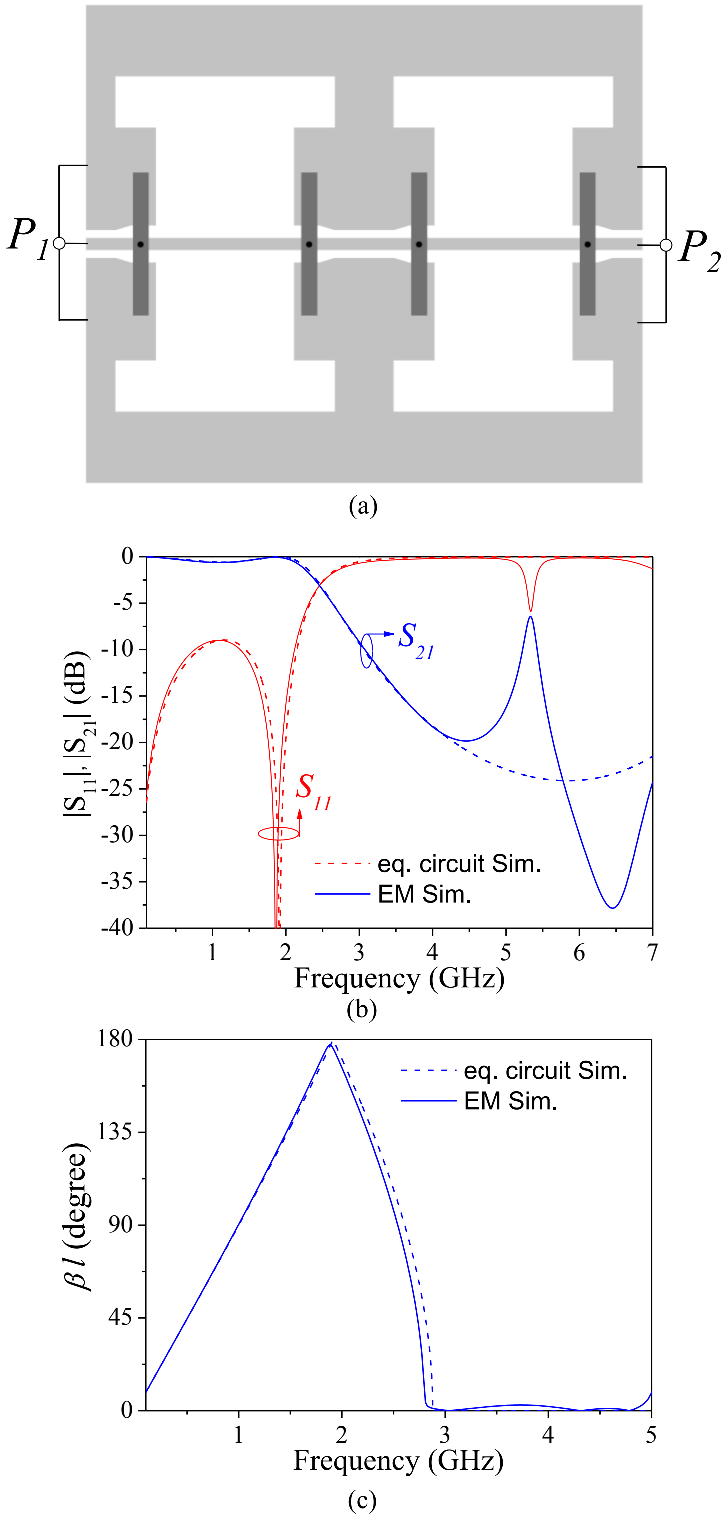

Fig. 3. Layout of the whole inverter, including two cells (a), transmission and reflection coefficients (b), and electrical length (c).

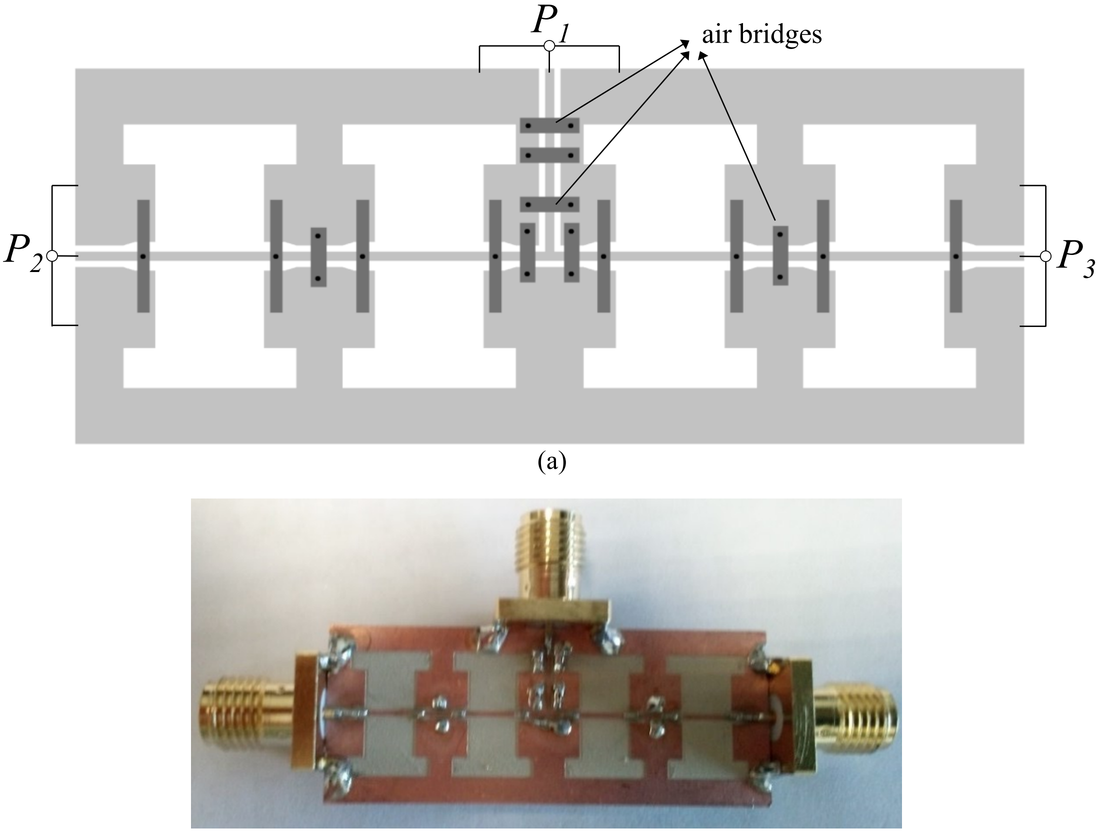

(a)

(b)

Fig. 4. Layout (a) and photograph (b) of the designed and fabricated power splitter.

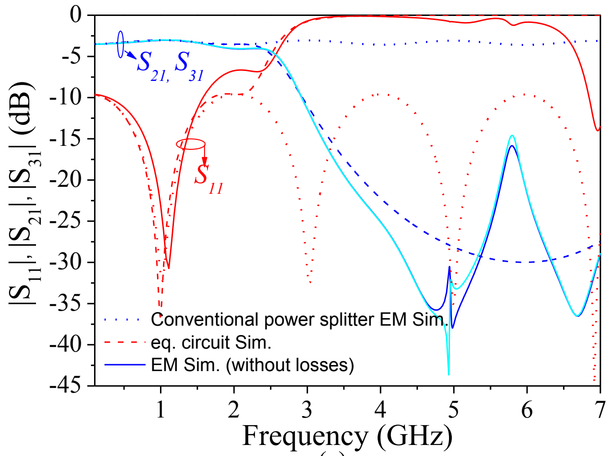

(a)

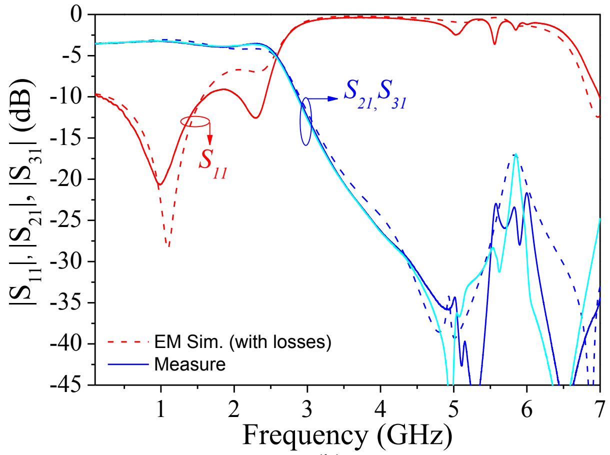

(b)

Fig. 5. Response of the splitter, including matching (S_{11}) and power splitting (S_{21} and S_{31}). (a) Circuit and lossless electromagnetic simulation; (b) lossy electromagnetic simulation and measurements. The lossless electromagnetic simulation of the conventional power splitter is also included in (a).